Journal of Applied Polymer Science

Sophorolipid-Induced Dimpling and Increased Porosity in Solvent-Cast Short-Chain Polyhydroxyalkanoate Films: Impact on Thermomechanical Properties

Richard D. Ashby, Daniel K.Y. Solaiman

U. S. Department of Agriculture, Eastern Regional Research Center, Agricultural Research Service, Wyndmoor, Pennsylvania 19038

Correspondence to: R.D. Ashby (E-mail: rick.ashby@ars.usda.gov)

ABSTRACT: Sophorolipids (SL; microbial glycolipids) were used as additives in solvent-cast short-chain polyhydroxyalkanoate (*sc*-PHA) films to enhance surface roughness and porosity. Poly-3-hydroxybutyrate (PHB), poly-(6%)-3-hydroxybutyrate-*co*-(94%)-3-hydroxyvalerate (PHB/V), and poly-(90%)-3-hydroxybutyrate-*co*-(10%)-3-hydroxyhexanoate (PHB/HHx) films were evaluated with up to 43 wt % of SL. Sophorolipid addition caused surface dimples with maximum diameters of 131.8 μm (PHB), 25.2 μm (PHB/V), and 102.8 μm (PHB/HHx). A rise in the size and number of pores in the polymer matrix also occurred in PHB and PHB/V films. Surface roughness and film porosity were visualized by scanning electron microscopy and quantitated using confocal microscopy by correlating the surface area (A′) to the scanned area (A) of the films. The phenotypic alterations of the films caused a gradual decline in tensile strength and modulus and increased the elongation to break. Reductions in the enthalpies of fusion (ΔH_f) in both the PHB (41% reduction) and PHB/HHx (36% reduction) films implied diminished crystallinity as SL concentrations increased. Over the same SL concentrations the Tan δ maxima shifted from 4 to 30°C and from 2 to 20°C in these respective films. These results provide a novel means by which *sc*-PHA properties can be controlled for new/improved applications. © 2014 Wiley Periodicals, Inc. J. Appl. Polym. Sci.† **2014**, *131*, 40609.

KEYWORDS: biopolymers and renewable polymers; films; mechanical properties; properties and characterization; surfactants

Received 31 October 2013; accepted 17 February 2014
DOI: 10.1002/app.40609

INTRODUCTION

Finite resources and pollution concerns have shifted focus from petroleum- to bio-based materials. As such, there is a mounting demand for development of renewable resources as feed stocks for biodegradable and biocompatible materials whose properties mimic if not surpass those of currently used products. Plastics are one particular area of concern as the majority of plastics on the market today are produced from petroleum-based precursors and do not conform to accepted biodegradation matrices. Over the past three decades bio-based plastics have gradually been developed as potential substitutes for petroleum-based plastics. Two of the most well-known bio-based polyester plastics are polylactic acid (PLA), which is chemically synthesized from fermentation-derived lactic acid typically through direct condensation reactions or through ring-opening polymerization reactions of lactide,[1] and polyhydroxyalkanoates (PHA), which are bacterial polyesters synthesized intracellularly by a number of diverse bacterial strains from a variety of substrates.[2]

Historically, PHAs [for chemical structure see Figure 1(A)] have been extensively studied and their physical properties developed for industrial applications where structural integrity is paramount.[3] More recently, they have been assessed either alone or as blends for their potential in the biomedical field[4–6] particularly for use as sutures[7] and tissue scaffolding materials.[8–10]

One vital characteristic for use of any material in clinical applications is "biocompatibility," a term used to indicate that the material itself, or any degradation products, do not cause an adverse immune response when introduced to the host organism. Poly-3-hydroxybutyrate (PHB) homopolymer is the most common form of the so-called short-chain PHA (*Sc*-PHA) and has been demonstrated to be a biodegradable and biocompatible thermoplastic with properties similar to polyethylene and polypropylene;[11] however, PHB has a relatively high crystal content

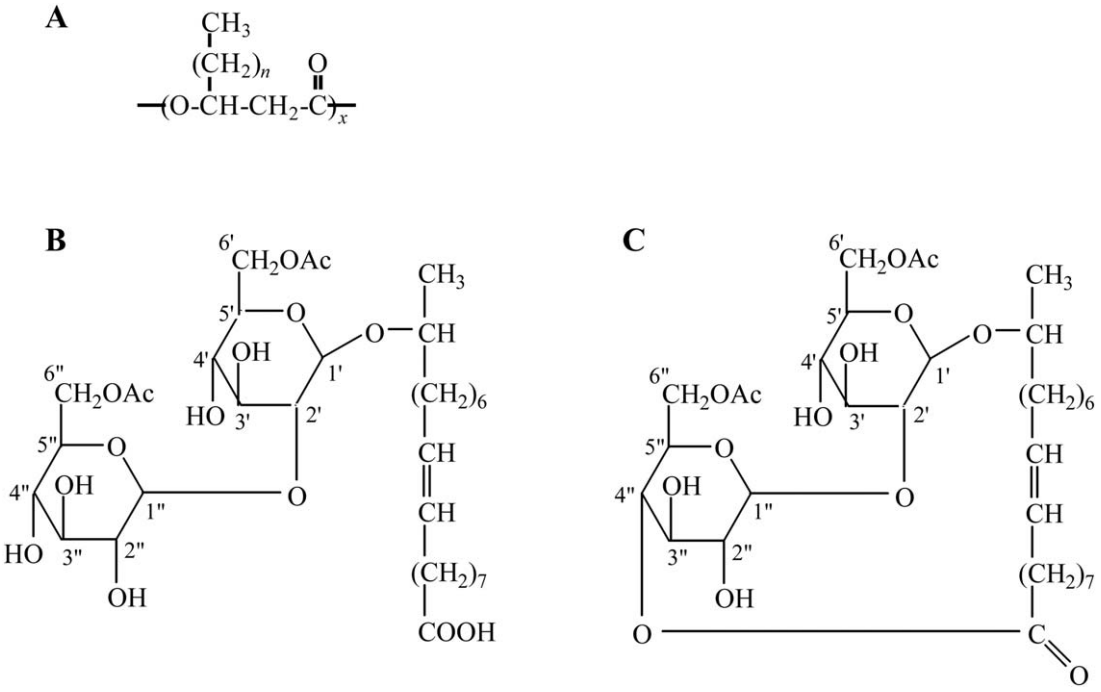

Figure 1. Chemical structures of poly-3-hydroxyalkanoate biopolymers (A; 3-hydroxybutyrate, $n = 0$; 3-hydroxyvalerate, $n = 1$; 3-hydroxyhexanoate, $n = 2$) and the 17-L-[2′-O-β-glucopyranosyl-β-D-glucopyranosyl]-oxy]-9-octadecenoic acid 6′,6″-diacetate sophorolipids in the free acid form (B) and the 1′,4″-lactone form (**C**).

making it brittle and imparting a relatively long degradation time under physiological conditions.[12] Degradation of PHB results in the generation of (R)-3-hydroxybutanoic acid (3HB), a ketone body normally found in trace amounts in the blood of healthy adults.[13] The typical presence of 3HB in the human body indicates that PHB and likely any other PHA types used in clinical applications (including other *sc*-PHA polymers such as poly-3-hydroxybutyrate-*co*-3-hydroxyvalerate, poly-3-hydroxybutyrate-*co*-4-hydroxybutyrate, and poly-3-hydroxybutyrate-*co*-3-hydroxyhexanoate) would naturally breakdown without eliciting an adverse immune response. In fact, many *sc*-PHA polymers have been assessed for biocompatibility in mammalian systems with little to no negative reaction.[7,14,15]

Sophorolipids (SL) are amphiphilic molecules that can be produced in high yields by many yeast strains primarily from the genus *Candida*.[16–19] They are synthesized as heterogenic mixtures (lactone vs. free acid) by fermentation from renewable substrates. SL are normally composed of a disaccharide (sophorose; 2-O-β-D-glucopyranosyl-β-D-glucopyranose) linked to a hydroxy fatty acyl moiety between the 1′ hydroxy group of the sophorose sugar and the ω or ω-1 carbon of the fatty acid [Figure 1(B,C)]. Typically, the fatty acid chain length varies between 16 and 18 carbons and may be saturated or unsaturated and the 6′ and 6″ hydroxy groups of the sophorose may be acetylated. These molecules are recognized to exhibit antibacterial,[20,21] antiviral,[22,23] and anticancer[24,25] activities and act as immunomodulators in mammalian systems.[26,27]

Historically, property control in PHA biopolymers focused on the successful inclusion of unique monomeric components into the polymer backbone,[2,28] blending[29–32] and the use of physical crosslinking protocols (e.g., irradiation, oxidation etc.).[33] The desire to develop a new method for property control in PHA polymers and effectively condition these *sc*-PHA polymers for enhanced applicability in bioremediation and biomedical applications was the driving force for this study. Sophorolipid successfully acted to enhance surface roughness (dimpling effect) and porosity in the PHA polymer films, which reduced polymer rigidity and imparted an antimicrobial quality to the films. This report focuses on the SL-induced control of the phenotypic alterations in the PHA polymer film matrices and the effects of these changes on the thermo-mechanical properties of the films.

EXPERIMENTAL

Materials

The microbial strains used in this work included *Pseudomonas oleovorans* NRRL B-14682 (used for the fermentative synthesis of PHB and poly-(6%)-3-hydroxybutyrate-*co*-(94%)-3-hydroxyvalerate (PHB/V)), which was obtained from the ARS Culture Collection (Peoria, IL) and shown to contain genes for *sc*-PHA synthesis,[34] and *Candida bombicola* ATCC 22214, a high-yield SL-producing yeast, which was purchased from American Type Culture Collection (Manassas, VA). Both microorganisms were stored at −80°C in Luria-Bertani (LB) broth (1% tryptone, 0.5% NaCl, 0.5% yeast extract) supplemented with 15% (v/v) glycerol as a cryopreservative. Poly-(90%)-3-hydroxybutyrate-*co*-(10%)-3-hydroxyhexanoate (PHB/HHx) was kindly supplied by Dr. Phil Green of Procter & Gamble (Cincinnati, OH). Glycerol (ReagentPlus™, ≥99.0%), glucose, oleic acid, and all media salts were purchased from Sigma Chemical Company (St. Louis,

MO). Levulinic acid (98+%) was purchased from Acros Organics (Geel Belgium). Bacto tryptone and bacto yeast extract (components of LB broth and Candida Growth Media; CGM) were purchased from Becton Dickinson (Sparks, MD).

Fermentations

PHB and PHB/V were synthesized by fermentation using *P. oleovorans* NRRL B-14682.[28] The biopolymers were separately produced in 10 l volumes in a 12 l capacity Bioflo 3000 bench-top fermenter (New Brunswick Scientific, Edison, NJ) using Medium E* (for media composition see Ref. 35) and a starting pH of between 6.9 and 7.0. PHB was synthesized from a 1% (w/v) glycerol feedstock while PHB/V was synthesized from a 0.5% glycerol : 0.5% levulinic acid (w/v) mixture.[28] All Medium E* salts and carbon sources were autoclaved separately as concentrated solutions and combined into the fermentation vessel to make 10 L of Media E* with a 1% carbon source concentration. The inoculum for each fermentation was prepared in LB broth by inoculating 50 mL of LB broth with 1.5 mL of *P. oleovorans* NRRL B-14682 from a frozen stock culture[36] and incubating the culture in a shake incubator at 30°C and 250 rpm. After 24 h the entire 50 mL culture was added to a 2 L Erlenmeyer flask containing 1 L of LB medium and incubated under the conditions described above. After 24 h the 1 L LB culture was aseptically centrifuged at 8000 × g, 4°C for 15 min to pellet the cells. The supernatant was discarded and the cell pellet was resuspended in 100 mL of Media E* from the 10 L fermentation vessel and the entire cell mass was added to the 10 L vessel. The 10 L fermentations were conducted at 30°C without pH control, impeller speed of 250 rpm and aeration at 3 standard liters per minute (SLPM) for 48 h.

Sophorolipid was also produced at the 10 L bench-top scale from *C. bombicola* ATCC 22214 grown on glucose and oleic acid.[16] The basal CGM (10% glucose, 1% yeast extract, 0.1% urea) was prepared, autoclaved to sterilize and the temperature was equilibrated to 26°C. Filter sterile oleic acid was added to the CGM as the lipid cosubstrate at a final concentration of 2% (v/v). One 50 mL frozen inoculum culture was thawed and used to inoculate the fermentation. The fermentation was conducted at a temperature of 26°C, an agitation rate set at 700 rpm, an air-flow rate of 2 L of air/min and no pH control. After 2 days, an additional 7.5% (w/v) of dry glucose and 2% (v/v) of oleic acid were added and the fermentation was allowed to proceed to 5 days when the fermentation was supplemented with an additional 1% (v/v) of oleic acid. The fermentation then continued for an additional 2 days until harvesting (total duration of the fermentation was 7 days).

Product Recovery

Short-chain PHA polymers were isolated and recovered by harvesting the bacterial cells by centrifugation (8000 × g, 4°C, 15 min) and drying the cell pellets by lyophilization to a constant weight. Both PHB and PHB/V were recovered from the lyophilized cells by chloroform extraction at 30°C overnight with shaking at 250 rpm. Insoluble cellular material was removed by filtration through Whatman #2 filter paper, and the chloroform was evaporated from the filtrate to concentrate the crude polymers. The crude polymers were precipitated a total of 3 times by dropwise addition to cold methanol. The polymers were recovered and dried *in vacuo* for 24 h.

Sophorolipid isolation and recovery was accomplished by lyophilizing the entire culture to dryness (~2 days). The dried residue was divided and placed into three 6 L Erlenmeyer flasks. Each fraction was extracted with excess ethyl acetate at room temperature for two days. The extract was filtered through Whatman No. 2 filter paper to remove any insoluble material (e.g., residual yeast cells). The remaining solids were washed two additional times with ethyl acetate to maximize recovery. The ethyl acetate fractions were combined, concentrated by evaporation and precipitated into 1 L aliquots of hexane to obtain the pure SL. The pure SL was recovered from the hexane by filtration (described above) and vacuum-dried in a desiccator to obtain a fine white to off-white powder.

sc-PHA and SL Characterization (Composition)

Repeat unit compositions of *sc*-PHA were determined by Proton–Nuclear Magnetic Resonance Spectroscopy (^{1}H-NMR) and Gas Chromatography/Mass Spectrometry (GC/MS) of the trimethylsilyl derivatives of the 3-hydroxymethyl esters as previously described.[28] The SL components were determined as described previously.[37]

Preparation of SL Impregnated PHB, PHB/V, and PHB/HHx Films

Sophorolipid-impregnated *sc*-PHA discs were prepared by weighing out 5 separate 0.5 g samples of PHB (set 1), PHB/V (set 2), and PHB/HHx (set 3) into separate 25 mL beakers (15 samples total). Sophorolipid was added to each set of beakers as follows: sample 1 = 0 SL, sample 2 = 50 mg SL, sample 3 = 125 mg SL, sample 4 = 250 mg SL, and sample 5 = 375 mg SL, resulting in SL concentrations of 0, 9, 20, 33, and 43 wt %. Ten milliliters of chloroform was added to each beaker and the contents were allowed to dissolve completely. The solvated contents of each beaker were poured into separate aluminum dishes (7.5 cm diameter) and the chloroform evaporated off at room temperature. The films were then placed under vacuum overnight to remove any residual solvent. Discs were punched out from the films using a standard paper hole-punch.

Analytical Procedures

Film surface morphologies and cross-sectioned porosity were visualized by scanning electron microscopy (SEM) and confocal microscopy (CM). Each sample was prepared for SEM analysis by dehydration in a graded series of ethanol solutions followed by critical point drying in liquid carbon dioxide. The dry film discs were mounted onto carbon adhesive tabs (Electron Microscopy Sciences, Hatboro, PA) and sputter-coated with a thin layer of gold. Digital images of the sample surfaces and cross-sections were collected with a Quanta 200 scanning electron microscope (FEI Company, Hillsboro, OR) operating in the high vacuum, secondary electron imaging mode. Duplicate samples were also stained with 0.5 mg/mL Nile Red and mounted in microwell dishes (MatTek Corporation, Ashland, MA) for imaging with a model IRBE optical microscope (Leica Microsystems, Bannockburn, IL) coupled to a model TCS-SP confocal system. Optical fluorescence was excited at 488 nm

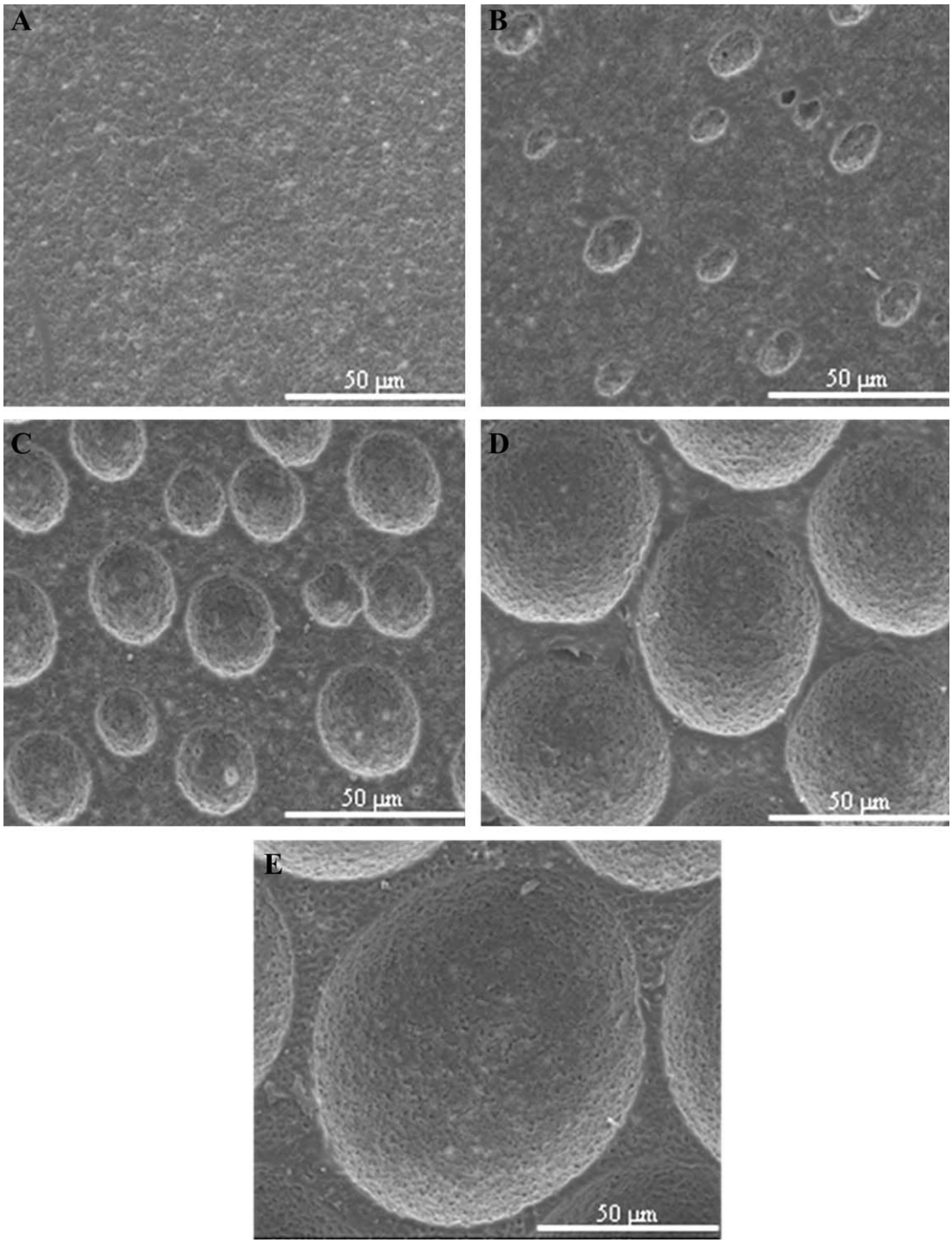

Figure 2. Scanning electron micrographs of the surface of PHB polymer films in the absence of SL (A) and in the presence of 9 wt % SL (B), 20 wt % SL (C), 33 wt % SL (D), and 43 wt % SL (E).

and emission between 580 and 620 nm was collected in a series of optical sections. The roughness of the film surfaces was computed from topographical images by correlating the surface area (A′) to the scanned area (A) of the film.

Thermal properties of each of the SL-impregnated PHB-, PHB/V-, and PHB/HHx-films were measured using a Pyris 1 Differential Scanning Calorimeter (DSC; Perkin-Elmer, Norwalk, CT) as described previously.[21] The initial heat for each of the DSC tests was from 0°C to 200°C at a ramp rate of 10°C/min from which the melting temperature (T_m) and enthalpies of fusion (ΔH_f) were determined. After quenching to −20°C, the second heat was performed up to 40°C (ramp rate = 10°C/min) and the glass transition temperatures (T_g) calculated from the second heat.

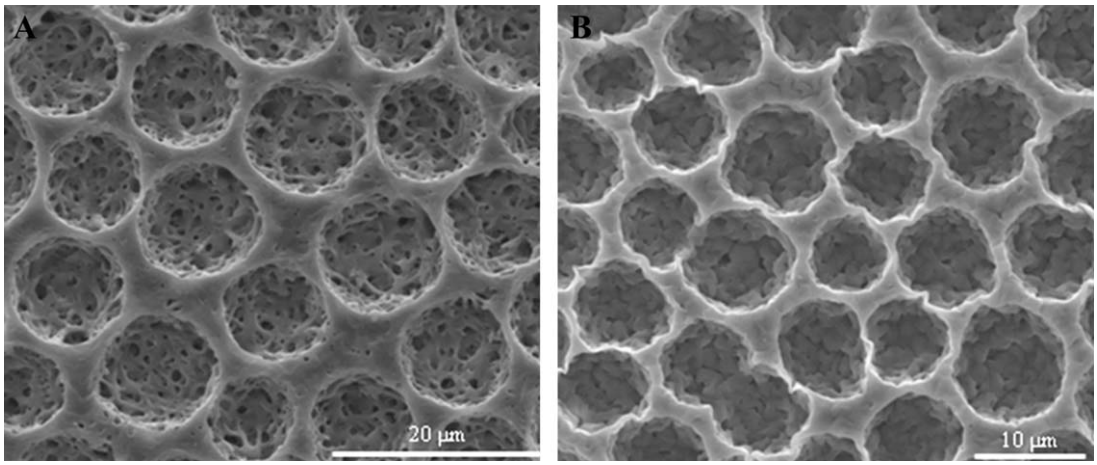

Figure 3. Scanning electron micrographs of the (A) PHB/HHx polymer film and (B) the PHB/V polymer film cast in the presence of 20 wt % SL.

Tensile testing of rectangular film specimens was performed as described previously[28] using an upgraded Instron mechanical property tester, model 1122 (Instron, Norwood, MA), and Testworks-4 data acquisition software (MTS Systems, Minneapolis, MN). Dynamic mechanical analyses (DMA) were conducted on a Rheometric RSA II Dynamic Analyzer (Piscataway, NJ) using Rheometric Scientific Orchestrator Software, version 6.5.7. Films were cut into rectangular strips (7 × 20 mm^2) and tested over a temperature range of −50 to 160°C (PHB) or −50 to 130°C (PHB/HHx) at a ramp rate of 10°C/min and a constant strain frequency of 10.0 rad/s.

RESULTS AND DISCUSSION

In a previous report we described the use of PHB and PHB/HHx as biopolymer supports in the slow release application of SL against *Propionibacterium acnes*, the causative bacteria of acne. In that study we found that dried solvent-cast films made from mixtures of PHA polymers and SL had a dimpled surface morphology as well as a porous matrix whose size and number varied based on SL concentration.[21] On the basis of this observation, we carried out a systematic study to evaluate the effect of SL inclusion on solvent-cast *sc*-PHA film morphology and subsequent properties. Films were solvent-cast from three distinct *sc*-PHA polymers (PHB, PHB/V, and PHB/HHx) with SL contents ranging from 0 to 43 wt %. SEM was used to visualize the individual film surfaces and the cross-sectioned film matrices. PHB was used as the primary polymer in this study because it is the most well-known polymer within the PHA family. Figure 2 shows the results of the SEM analyses of the PHB film surfaces. In the absence of SL the PHB film surface was relatively smooth with no hint of surface irregularities [Fig. 2(A)]; however, as the SL concentration increased to 9 wt %, noticeable dimples began to appear that had an average diameter of 17.5 μm [Figure 2(B)]. As the SL concentration within the films continued to increase the average dimple diameters increased by 79% [between 9 and 20 wt % SL; Figure 2(C)], by 164% [between 20 and 33 wt % SL; Figure 2(D)], and by 59% [between 33 and 43 wt %; Figure 2(E)]. The same tendencies were seen in the PHB/V and PHB/HHx polymer films although the surface irregularities in the PHB/V and PHB/HHx films resembled pitted structures rather than the dimples seen in the SL-impregnated PHB films. In fact, at 20 wt % SL the surfaces of the PHB/V and PHB/HHx films were similar to each other (Figure 3) but different than the SL-containing PHB homopolymer [c.f. the images in Figures 3 to 2(C)]. A progressive comparison of the dimple diameters from each of the 3 SL-impregnated PHA polymer films is shown in Figure 4. It is apparent that the PHB films maintained the largest dimples at equivalent SL concentrations. At 43 wt % SL the PHB films had a maximum diameter of 131.8 μm while PHB/HHx demonstrated the second largest average dimple diameter at 102.8 μm. Poly-(6%)-3-hydroxybutyrate-*co*-(94%)-3-hydroxyvalerate showed a more linear increase in dimple diameter as the SL content increased and only reached a maximum diameter of 25.2 μm at 43 wt % SL.

CM was used to quantitate the surface roughness of the films by dividing the surface area (A′) of the films by the scanned area (A) of the films. In a perfectly flat film, devoid of all irregularities, the A′/A value would equal one. Any increase in the A′/A ratio above one is indicative of an increase in the surface

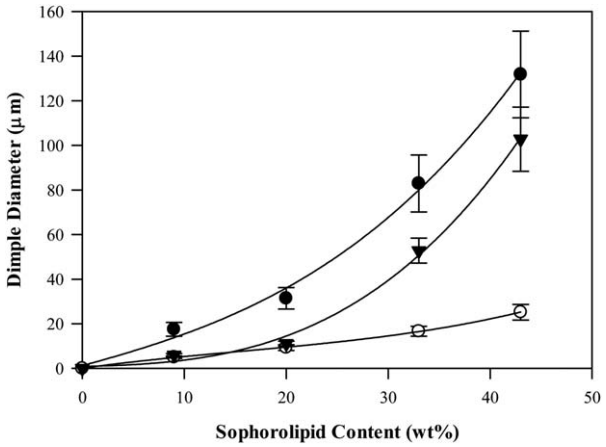

Figure 4. Comparative dimple diameters for PHB (●), PHB/V (○) and PHB/HHx (▼) polymer films cast in the presence of up to 43 wt % SL.

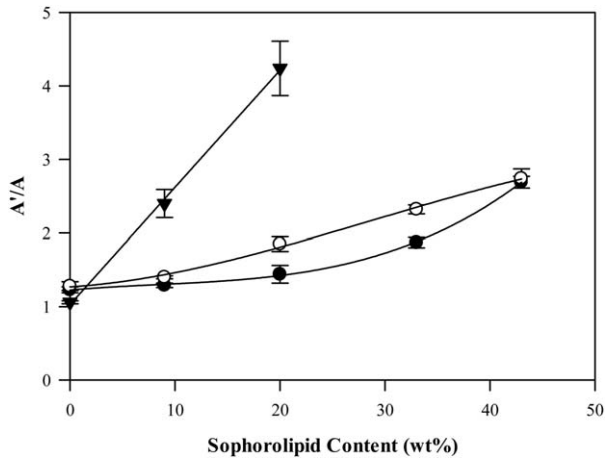

Figure 5. Comparative film surface roughness measured by confocal microscopy correlating the surface area of the films (A′) to the scanned area of the films (A); PHB (●), PHB/V (○), and PHB/HHx (▼).

roughness of the film. Results from confocal imagery (A′/A) are shown in Figure 5. The PHB film surface in the absence of SL demonstrated an average A′/A value of 1.23 ± 0.04 ($n = 3$). As the SL content in the PHB films increased, the A′/A values also increased to a maximum value of 2.69 ± 0.08 ($n = 3$) at 43 wt % SL. These results indicated that SL content was the primary factor involved in the increased surface roughness of the PHB films. Surface roughness results for the PHB/V films mimicked those of PHB however; at 20 and 33 wt % SL the A′/A ratios in the SL-laden PHB/V films were 28% and 24% greater, respectively than in the equivalent PHB films. In contrast, the starting PHB/HHx film surface showed an A′/A ratio of 1.06 ± 0.02 ($n = 3$), which was smaller than that from PHB indicating that in the absence of SL the PHB/HHx film was smoother than the PHB counterpart. The PHB/HHx film surface reached a maximum A′/A value that was approximately 58% larger (A′/A $= 4.24 \pm 0.37$; $n = 3$) than PHB with approximately half (20 vs. 43 wt %) of the SL present. These results were attributed to an increase in the number and depth of the dimples in the PHB/HHx film surface at 20 wt % SL [c.f. Figures 2(C) and 3(A)]. While the PHB films containing 43 wt % SL had larger dimples, fewer numbers and a reduced dimple depth resulted in a smoother surface than the PHB/HHx at a SL-load of 20 wt %. Above 20 wt % SL the A′/A ratio of the PHB/HHx film surfaces declined to 3.00 ± 0.26 ($n = 3$) at 33 wt % SL and finally to 2.69 ± 0.10 ($n = 3$) at 43 wt % SL, indicative of dimple coalescence at elevated SL-loads.

Cross-sectioning was performed on each of the SL-impregnated PHA polymer films to assess the effects of SL on the porosity within the polymer matrices. The results from the PHB polymers can be seen in Figure 6. PHB homopolymers in the absence of SL showed a uniform matrix devoid of pores. At a SL-load of 9 wt % very small pores began to appear throughout the entire cross-section; however, it was not until a SL-load of 20 wt % that obvious pores were present in the top quarter of the film. At a SL concentrations of 33 and 43 wt % there were pores scattered throughout the entire PHB film. The porosity of the films made from PHB/V resembled the results from PHB (data not shown) in that pores were not visible throughout the film matrix until 33 wt % SL was included. This was not the case for SL-impregnated PHB/HHx films. In the PHB/HHx films porosity was not uniformly distributed across the entire matrix but only a few pores were visible even at 43 wt % SL (data not shown).

In a previous report, Baccile et al.[38] reported that the self-assembly of acidic SLs was dependent upon pH variations and the resulting differences in the degree of ionization in an aqueous environment. In that report it was determined that at low ionization values ($pH < 5$), SL concentration drives the self-assembly process and micelles are generally identified as non-ionic with curvature that is dependent on the SL concentration. At mid-ionization levels ($5 < pH < 8$) the formation of COO^- groups introduced negative charges at the micellar surface, which increased micellar curvature while at higher ionization levels ($pH > 8$) the micelles favored the formation of large tubular aggregates above 100 nm. In the present study, chloroform was utilized as the solvent for casting SL-impregnated PHA polymer films. Selective solubility of the postcasted films in methanol revealed that the SL could be effectively removed from the films thereby signifying that the SL did not seem to be involved in surfactant-polymer complexation reactions. The dimpling and pore formation was more likely due to phase separation in chloroform of the SL and PHA polymers as the films dried. This phenomenon explains the increased porosity towards the top of the film matrices and the formation of larger dimples upon coalescence of SL at the PHA polymer film surface as the SL concentrations increased.

Increased porosity had a profound effect on the tensile and thermo-mechanical properties of the different PHA polymer films. The tensile strength of any material is only as great as its weakest point. In each of the PHA polymers tested, the tensile strength [reported as peak stress; Figure 7(A)] and modulus [Figure 7(B)] showed an inverse relationship. As the SL concentration in the films increased the tensile strength and modulus of the polymer films decreased. These results are due, at least in part, to the increase in the number and size of the pores brought about by increasing SL concentrations. Although no X-ray diffraction data was obtained in this study (hard evidence of changes in crystallinity), a second contributing factor in decreased tensile strength and modulus may be a SL-induced disruption of the polymer lattice within the polymer matrix. Data showed that the tensile strength of the PHB-based polymer films reduced by 65% from 26.8 to 9.3 MPa over the range of 0 to 43 wt % SL (a 1.5% decrease in tensile strength per percent SL included in the PHB film). Similarly, tensile strength of both PHB/V and PHB/HHx decreased over the range of SL concentrations. The PHB/V tensile strength dropped by 56% (a 1.1% decrease per % SL included in the film) and that of PHB/HHx was reduced by 49% (a 1.3% decrease per % SL included in the film). Since the PHB/HHx films showed very little pore formation upon inclusion of SL, it is likely that the reduction in tensile strength in the PHB/HHx films was based primarily on an increased amorphous character of the films at higher SL concentrations.

Modulus is a general indicator of the stiffness of a polymer film. In the present study, the PHB polymer film without SL inclusion exhibited a modulus of 1390 MPa, which was 168%

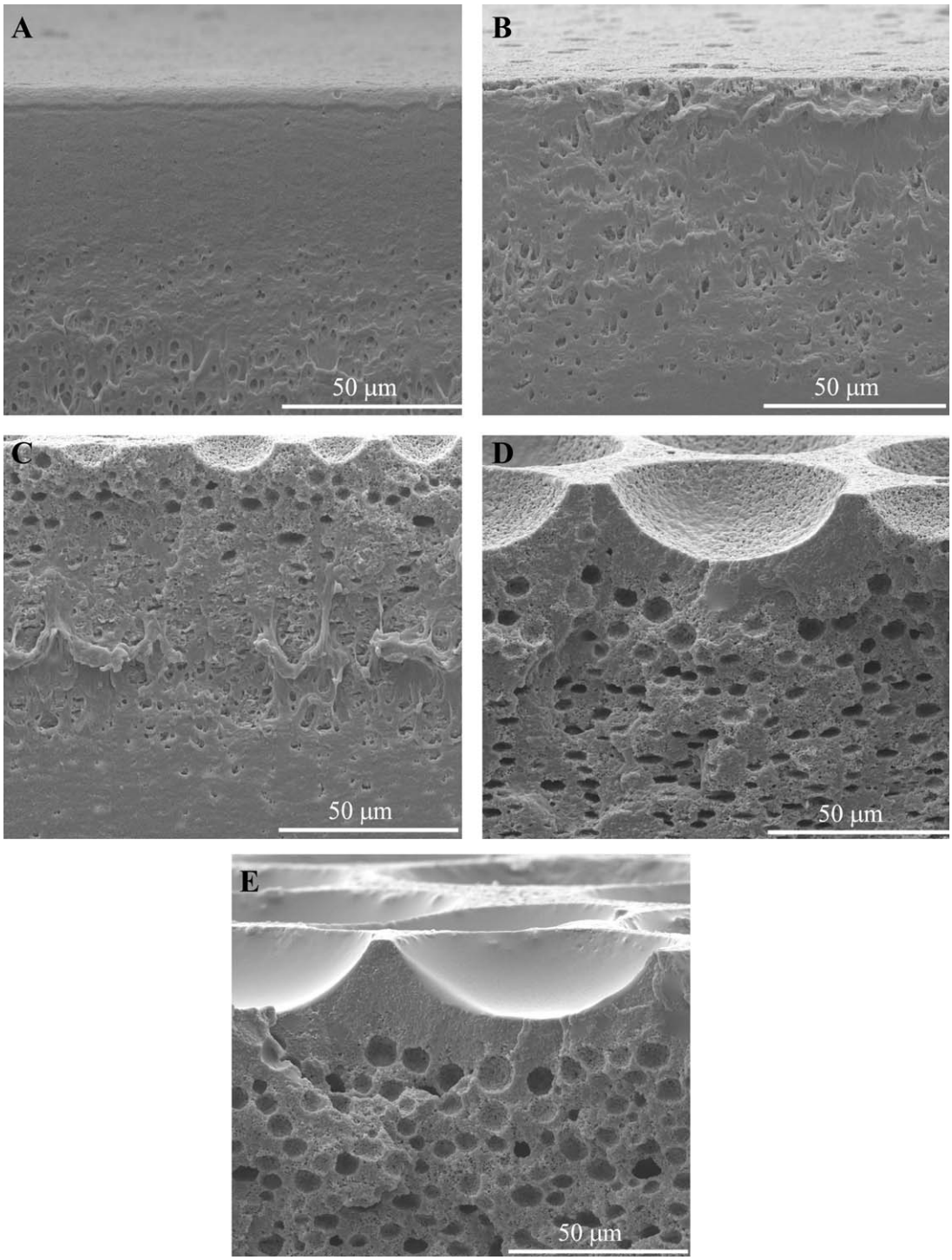

Figure 6. Scanning electron micrographs of the cross-sections of PHB polymer films (A) in the absence of SL and (B) in the presence of 9 wt % SL, (C) 20 wt % SL, (D) 33 wt % SL, and (E) 43 wt % SL.

and 251% larger than the modulus of PHB/HHx and PHB/V, respectively. These results are proof that, as expected, in the absence of SL the PHB films were naturally stiffer than either the PHB/V or PHB/HHx films. Over the range of SL concentrations the modulus from the PHB films decreased to 457.9 MPa, a 67% reduction, while the modulus from PHB/V and PHB/HHx decreased by 45% to 217.3 MPa and by 53% to 244.1 MPa, respectively. In all cases, elevated SL concentrations resulted in a lower modulus regardless of the specific polymer signifying a SL-induced reduction in the stiffness of the films.

In contrast to the tensile strength and modulus results, SL acted to increase the elongation to break in the PHB/HHx and PHB/V polymer films [Figure 7(C)]. In fact, the elongation to break in the films increased by 150% (from 154.5 to 386.9% between 0

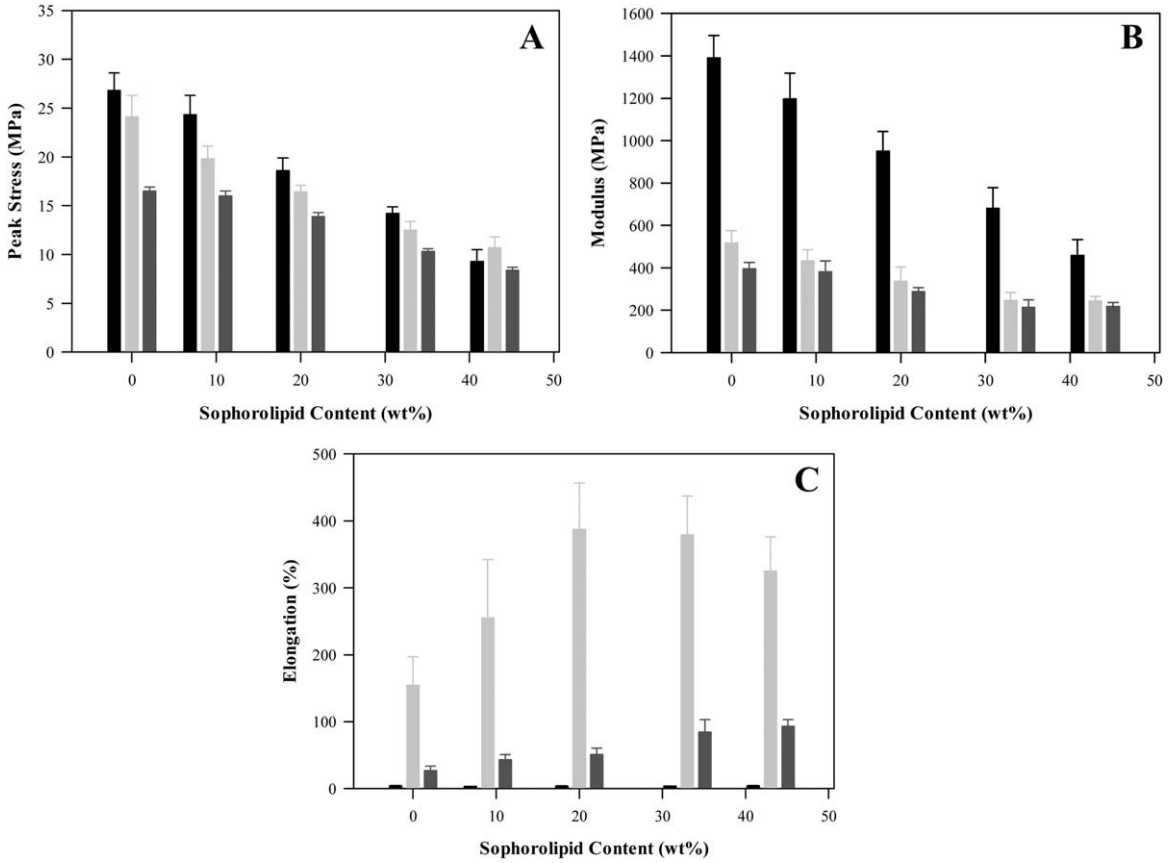

Figure 7. Effect of increasing SL content on the (A) tensile strength, (B) modulus, and (C) elongation of PHB polymer films (■), PHB/V polymer films (■), and PHB/HHx polymer films (■).

and 20 wt % SL) and 247% (from 26.8 to 93.1% between 0 and 43 wt % SL) in the PHB/HHx and PHB/V films, respectively. Above 20 wt % SL the elongation to break in the PHB/HHx films began to gradually decline. In contrast, the elongation to break in the PHB-based films remained relatively constant at $3.8 \pm 0.5\%$ regardless of the SL content of the films. It appeared that the SL had a plasticizing effect on the films. While SL caused an across-the-board drop in tensile strength of the PHA films, it also helped to reduce the stiffness of the PHA polymer films and improve the elastomeric properties of the PHB/V and PHB/HHx polymer films.

Differential scanning calorimetry (DSC) revealed that SL concentration had a modest effect on the melting temperatures (T_m) and glass transition temperatures (T_g) of the polymer films but increased SL content did result in a steady decrease in the enthalpies of fusion (ΔH_f; data for PHB and PHB/HHx are shown in Table I). The T_m of the PHB films dropped 7°C and that of the PHB/HHx films dropped 4°C over the entire span of SL concentrations tested. The T_g values were even more stable, changing less than 1°C between 0 and 43 wt % SL. The enthalpies of fusion (ΔH_f; indicative of the amount of energy necessary to melt the polymer) of the PHB and PHB/HHx polymer films did noticeably decrease as the SL content in the films rose. PHB, whose crystallinity has been reported as being between 50 and 60%,[39,40] showed a ΔH_f of 81.2 ± 2.3 J/g ($n = 3$) in the absence of SL. As the SL content increased, the ΔH_f values decreased by 42% to a final value of 47.5 ± 1.5 J/g ($n = 3$) at a SL-load of 43 wt %. This indicated that less energy was needed to melt the SL-containing films, suggesting a reduced crystallinity. The same trend was noticed with the PHB/HHx films. Poly-3-hydroxybutyrate-*co*−3-hydroxyhexanoate typically maintains a more amorphous quality than PHB. This was noted by the reduced ΔH_f value (36.7 ± 6.6 J/g) in the absence of SL as compared to the PHB film. The same reductive tendency was observed in the ΔH_f values from the SL-laden PHB/HHx polymer films as in the PHB polymer films.

Dynamic mechanical analysis (DMA) was performed on the series of PHB and PHB/HHx polymer films. The storage modulus (E'), a measurement of the stored energy in the polymer films, can be a representation of the stiffness or the elasticity of the material. The E' trends for PHB and PHB/HHx at 0 and 43 wt % SL are shown in Figure 8(A). In the absence of SL the E' of the PHB film decreased relatively linearly from −50°C to ~75°C at which point the film entered the highly viscoelastic regime. At 105°C the PHB film continued to soften and show a very low modulus by 150°C. In contrast, the PHB film containing 43 wt % SL demonstrated a more obvious primary transition beginning at 7°C and continuing until ~70°C where it too entered the "rubbery" regime. PHB/HHx is naturally more viscoelastic than PHB due to its

Table I. Thermal Properties of PHB and PHB/HHx Films ($n = 3$) in the Presence of up to 43 wt % SL As Measured by Differential Scanning Calorimetry (DSC)

PHA film	SL content (wt %)	T_m (°C)	T_g (°C)	ΔH_f (J/g)
PHB	0	173	4.2	81.2 ± 2.3
	9	170	4.3	71.6 ± 1.1
	20	167	4.6	61.7 ± 2.2
	33	167	4.6	57.3 ± 2.7
	43	166	4.6	47.5 ± 1.5
PHB/HHx	0	134	1.1	36.7 ± 6.6
	9	134	1.7	30.1 ± 3.5
	20	130	1.6	27.2 ± 2.6
	33	132	1.8	23.0 ± 3.3
	43	130	1.8	23.5 ± 6.6

copolymeric nature. This was evident by the temperatures at which the PHB/HHx films began their α-transitions. In the absence of SL the α-transition began at −30°C and continued to 17°C. The inclusion of 43 wt % SL resulted in a shift in the start of the α-transition to −15°C and continuing to 25°C.

In contrast to the storage modulus, the loss modulus (E'') represents the energy of a material that is dissipated as heat. The E'' values for PHB and PHB/HHx in the absence and in the presence of 43 wt % SL are seen in Figure 8(B). The E'' maxima for both of the PHB/HHx film samples (regardless of the presence of SL) was at −7°C; however, there appeared to be a bimodal peak in the E'' of the SL-containing PHB/HHx sample. In contrast, the maxima for the PHB-based films increased from −2°C in the absence of SL to 28°C in the presence of 43 wt % SL. This result indicated that higher SL contents caused a higher temperature requirement for maximum energy dissipation in the PHB films. This was not true for the PHB/HHx films where maximum energy dissipation occurred at the same temperature regardless of SL concentration. Tan δ values are measurements of the damping or the dissipation of energy within a material. It is a representation of the ratio of the loss modulus to the storage modulus (E''/E') and is a good indicator of the midpoint between the "glassy" and "rubbery" states of a polymer. The Tan δ maximum can be used to represent the glass transition temperature (T_g) of a material; however, because DSC measures heat flow to and from a specimen relative to an inert reference and DMA measures mechanical stiffness and energy absorption of a specimen by applying an oscillating mechanical stress and strain within the viscoelastic

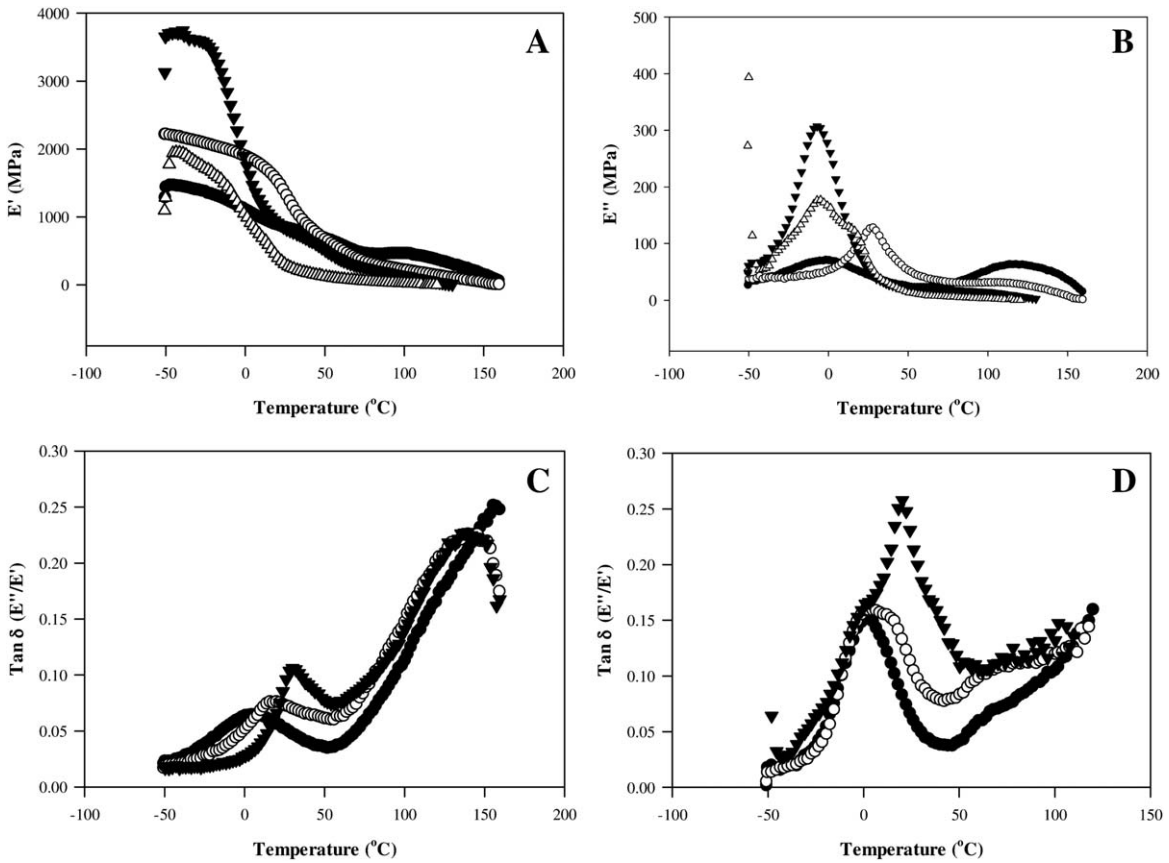

Figure 8. Dynamic mechanical analysis (DMA) results depicting the effect of increasing SL contents on the storage moduli (E'; A) and the loss moduli (E''; B) of PHB and PHB/HHx films (PHB films in the absence of SL (●), PHB films in the presence of 43 wt % SL (○), PHB/HHx films in the absence of SL (▼), and PHB/HHx films in the presence of 43 wt % SL (△). Also, the effect of SL on the Tan δ (E''/E') values from PHB (C) and PHB/HHx (D) polymer films in the absence of SL (●) and in the presence of 20 wt % (○) and 43 wt % SL (▼).

region, it is not uncommon to see as much as a 25°C difference in T_g data from DSC to DMA data reported as the peak of Tan δ.[41] The Tan δ plots of PHB and PHB/HHx in the absence and presence of SL are shown in Figure 8(C,D), respectively. In the absence of SL the Tan δ maximum for PHB was 4°C, identical to the T_g value measured by DSC. As the SL concentration increased in the PHB film to 20 wt %, the Tan δ maximum increased to 20°C and ultimately to 30°C at 43 wt % SL. Additionally, as the SL content increased in the PHB films, the height of the Tan δ peaks increased, which is an indicator of an increased amorphous content in the system.[42] The Tan δ of the PHB/HHx film in the absence of SL was 2°C, identical to the T_g value measured by DSC. In contrast to the PHB system, the PHB/HHx films in the presence of 20 wt % SL maintained a Tan δ maximum of 2°C but began to demonstrate a bimodal distribution within the peak, which was exacerbated in the presence of 43 wt % SL. In fact, at 43 wt % SL the Tan δ maximum increased to 20°C and maintained a height that was greater than the peak heights representing the 0 and 20 wt % PHB/HHx films indicative once again of increased amorphous content.

CONCLUSIONS

Previous reports have demonstrated that while surface properties of *sc*-PHA films are favorable for attachment and proliferation of tissue culture cells,[43] rougher film surfaces and increased porosity improve scaffolding properties for tissue growth.[44] In addition, PHB implants have been successfully used but are known to cause minor tissue responses in mammalian systems, which are attributed to the rigidity of the PHB that exerts a mechanical stimulus to the tissues surrounding the implant.[45,46] In this study, we were able to control the surface roughness and porosity of the *sc*-PHA polymer films through the addition of varying concentrations of SL. These phenotypic variations in the *sc*-PHA polymer films changed the thermo-mechanical properties by inducing a SL concentration-dependent reduction in the tensile strength and modulus (stiffness) and increase in the elongation behavior of each composite film. DMA results indicated that, in addition to increased porosity, these changes may be due to an amplified amorphous quality imparted to the *sc*-PHA polymer matrices by the SLs resulting in less rigid, more pliable *sc*-PHA polymers films. Therefore, in the correct SL/polymer ratios, *sc*-PHA polymers can be produced that may be strong enough to serve in tissue scaffolding applications yet malleable enough to eliminate the mechanical stimulus that rigid *sc*-PHA (*e.g.*, PHB) exerts to tissues when used as scaffolding materials for tissue implants. If PHA materials can be designed that perform as well or better than currently used materials in clinical applications and be combined with the slow release of antimicrobials and immunomodulators, such as SL, these materials may further broaden the application-base for *sc*-PHA and be an additional impetus for the discovery of bio-based replacements for petroleum-based polymers.

ACKNOWLEDGMENTS

The authors thank Peter Cooke, David Coffin, Nick Latona, Nicole Cross, and Bun Hong Lai for their technical assistance throughout this study.

REFERENCES

1. Södergård, A.; Stolt, M. In Poly(lactic acid): Synthesis, Structures, Properties, Processing, and Applications; Auras, R.; Lim, L.-T.; Selke, S. E. M.; Tsuji, H., Eds.; Wiley: Hoboken, **2010**; pp 27.
2. Steinbüchel, A.; Valentin, H. E. *FEMS Microbiol. Lett.* **1995**, *128*, 219.
3. Philip, S.; Keshavarz, T.; Roy, I. *J. Chem. Technol. Biotechnol.* **2007**, *82*, 233.
4. Wu, Q.; Wang, Y.; Chen, G. Q. *Artif. Cells Blood Subst. Immobil. Biotechnol.* **2009**, *37*, 1.
5. Valappil, S. P.; Misra, S. K.; Boccaccini, A. R.; Roy, I. *Expert Rev. Med. Devices* **2006**, *3*, 853.
6. Brigham, C. J.; Sinskey, A. *J. Int. J. Biotechnol. Wellness Ind.* **2012**, *1*, 53.
7. Shishatskaya, E. I.; Volova, T. G.; Puzyr, A. P.; Mogilnaya, O. A.; Efremov, S. N. *J. Mater. Sci. Mater. Med.* **2004**, *15*, 719.
8. Misra, S. K.; Valappil, S. P.; Roy, I.; Boccaccini, A. R. *Biomacromolecules* **2006**, *7*, 2249.
9. Asran, A. S.; Razghandi, K.; Aggarwal, N.; Michler, G. H.; Groth, T. *Biomacromolecules* **2010**, *11*, 3413.
10. Chen, G. Q.; Wu, Q. *Biomaterials* **2005**, *26*, 6565.
11. Chodak, I. In Degradable Polymers Principles and Applications, 2nd ed.; Scott, G., Ed.; Kluwer Academic: Dordrecht, **2002**; pp 295.
12. Arcana, I. M.; Sulaeman, A.; Pandiangan, K. D.; Handoko, A.; Ledyastuti, M. *Polym. Int.* **2006**, *55*, 435.
13. Williams, S. F.; Martin, D. P. In Biopolymers; Doi, Y.; Steinbuchel, A., Eds.; Wiley/VCH Verlag: Weinheim, **2002**; Vol. *4*, pp 91.
14. Qu, X. H.; Wu, Q.; Zhang, K. Y.; Chen, G. Q. *Biomaterials* **2006**, *27*, 3540.
15. Shishatskaya, E. I.; Volova, T. G.; Gitelson, I. I. *Dokl. Biol. Sci.* **2002**, *383*, 109.
16. Ashby, R. D.; Solaiman, D. K. Y.; Foglia, T. A. *Biotechnol. Lett.* **2008**, *30*, 1093.
17. Hommel, R. K.; Huse, K. *Biotechnol. Lett.* **1993**, *33*, 853.
18. Konishi, M.; Fukuoka, T.; Morita, T.; Imura, T.; Kitamoto, D. *J. Oleo. Sci.* **2008**, *57*, 359.
19. Kurtzman, C. P.; Price, N. P. J.; Ray, K. J.; Kuo, T. M. *FEMS Microbiol. Lett.* **2010**, *311*, 140.
20. Lang, S.; Katsiwela, E.; Wagner, F. *Fett. Wiss. Technol-Fat Sci. Technol.* **1989**, *91*, 363.
21. Ashby, R. D.; Zerkowski, J. A.; Solaiman, D. K. Y.; Liu, L. S. *New Biotechnol.* **2011**, *28*, 24.
22. Shah, V.; Doncel, G. F.; Seyoum, T.; Eaton, K. M.; Zalenskaya, I.; Hagver, R.; Azim, A.; Gross, R. *Antimicrob. Agents Chemother.* **2005**, *49*, 4093.
23. Gross, R. A.; Shah, V. World Pat. WO2007US63701 (**2007**).
24. Chen, J.; Song, X.; Zhang, H.; Qu, Y. B.; Miao, J. Y. *Appl. Microbiol. Biotechnol.* **2006**, *72*, 52.
25. Fu, S. L.; Wallner, S. R.; Bowne, W. B.; Hagler, M. D.; Zenilman, M. E.; Gross, R.; Bluth, M. H. *J. Surg. Res.* **2008**, *148*, 77.

26. Bluth, M. H.; Kandil, E.; Mueller, C. M.; Shah, V.; Lin, Y. Y.; Zhang, H.; Dresner, L.; Lempert, L.; Nowakowski, M.; Gross, R.; Schulze, R.; Zenilman, M. E. *Crit. Care Med.* **2006**, *34*, 188.
27. Bluth, M. E.; Fu, S. L.; Fu, A.; Stanek, A.; Smith-Norowitz, T. A.; Wallner, S. R.; Gross, R. A.; Nowakowski, M.; Zenilman, M. E. *J. Aller. Clin. Immunol.* **2008**, *121*(Supple 1), S2.
28. Ashby, R. D.; Solaiman, D. K. Y.; Strahan, G. D.; Zhu, C.; Tappel, R. C.; Nomura, C. T. *Bioresour. Technol.* **2012**, *118*, 272.
29. Ashby, R. D.; Solaiman, D. K. Y.; Foglia, T. A. *Biomacromolecules* **2005**, *6*, 2106.
30. Ashby, R. D.; Solaiman, D. K. Y.; Foglia, T. A. *J. Ind. Microbiol. Biotechnol.* **2002**, *28*, 147.
31. Yu, L.; Dean, K.; Li, L. *Prog. Polym. Sci.* **2006**, *31*, 576.
32. Chen, G. Q.; Luo, R. C. In Biodegradable Polymer Blends and Composites from Renewable Resources; Yu, L., Ed.; Wiley: Hoboken, **2009**; pp 191.
33. Hoefer, P. *Front. Biosci.* **2010**, *15*, 93.
34. Solaiman, D. K. Y.; Ashby, R. D. *Curr. Microbiol.* **2005**, *50*, 329.
35. Brandl, H.; Gross, R. A.; Lenz, R. W.; Fuller, R. C. *Appl. Environ. Microbiol.* **1988**, *54*, 1977.
36. Ashby, R. D.; Solaiman, D. K. Y.; Foglia, T. A.; Liu, C.-K. *Biomacromolecules* **2001**, *2*, 211.
37. Nuñez, A.; Ashby, R.; Foglia, T. A.; Solaiman, D. K. Y. *Chromatographia* **2001**, *53*, 673.
38. Baccile, N.; Babonneau, F.; Jestin, J.; Pehau-Arnaudet, G.; Van Bogaert, I. *ACS Nano* **2012**, *6*, 4763.
39. Bluhm, T. L.; Hamer, G. K.; Marchessault, R. H.; Fyfe, C. A.; Veregin, R. P. *Macromolecules* **1986**, *19*, 2871.
40. Kunioka, M.; Tamaki, A.; Doi, Y. *Macromolecules* **1989**, *22*, 694.
41. Perkin Elmer, Dynamic Mechanical Analysis: A Beginners Guide. http://www.perkinelmer.com/CMSResources/Images/4474546GDE_IntroductionToDMA.pdf.
42. Turi, E. A. Thermal Characterization of Polymeric Materials, 2nd ed.; Academic Press: Brooklyn, **1997**; Vol. *1*, pp 980.
43. Chan, R. T. H.; Marcal, H.; Ahmed, T.; Russell, R. A.; Holden, P. J.; Foster, L. J. R. *Polym. Int.* **2013**, *62*, 884.
44. Galperin, A.; Long, T. J.; Ratner, B. D. *Biomacromolecules* **2010**, *11*, 2583.
45. Lobler, M.; Sass, M.; Kunze, C.; Schmitz, K.-P.; Hopt, U. T. *J. Biomed. Mater. Res.* **2002**, *61*, 165.
46. Unverdorben, M.; Spielberger, A.; Schywalsky, M.; Labahn, D.; Hartwig, S.; Schneider, M.; Lootz, D.; Behrend, D.; Schmitz, K.; Degenhardt, R.; Schaldach, M.; Vallbracht, C. *Cardiovasc. Intervent. Radiol.* **2002**, *25*, 127.